Nonlinear Seismic Analysis on Joint of Concrete-filled Square Steel Tube Column and H-shaped Steel Beam

S. Yan, L.F. Shao, Y.G. Zhang, J.Z. Fu
School of Civil Engineering, Shenyang Jianzhu University, Shenyang, Liaoning, China

B.H. Qi, F.X. Liu
Building Research Institute, Angang Construction Group, Anshan Liaoning, China

SUMMARY:
The composite frame structures with concrete-filled square steel tube column and H-shaped steel beam have been becoming popular in China for its great seismic performance and advantages in construction. However, most of attentions have been paid to the capacities of columns and beams, and less to the joints, especially the seismic performance of the joint. A nonlinear finite element analysis (FEA) for the kind of joint was performed in the paper by using the software ANSYS based on a real engineering project of Dagongpu in Anshan city, Liaoning province, China, focusing on the influence of parameters of connection of panel point plate on the seismic performance of the joint. The joints were deformed with cyclic loading to develop the hysterestic loop, limit load-bearing capacity, and failure modes. The results of the numerical simulation showed that the joints had great seismic performance if the connections were suitably designed.

Keyword: Concrete-filled square steel tube; Beam-column join; Finite element method (FEM); cycle loading.

1. INTRODUCTION

Along with high-level and the extra-high building had been built rapidly around the world, frame structures composed of concrete-filled steel tube (CFST) column and steel beam have gradually become the major form in the field of building, especially the CFST column has been widely concerned by its advantages of regular shape and easy work.

For the frame system of composite structure of the CFST column and steel beam, it is extremely important to study its force performance and failure mode. Scholars from various countries have also done a lot of research and experimentation, mostly concentrated on the performance of a single component, but for the joints performance, the research is still relatively less.

In this paper, based on an actual project, we will numerically analyze the joint of the CFST column and H-shaped steel beam. In this actual project, the joint is a style with the clapboard passing through. According to self-characteristic of the joint, we use ANSYS to simulate this joint and to perform finite element analysis. We try to understand the force performance and failure mode of the type of joints, analyze the seismic performance by change the partitions and other parameters of that type of joints, and put forward some advice for design.

Since the 1980s, scholars at home and abroad have been analyzing in the composite structure of CFST column and steel beam. In 2004, China Engineering Construction Standardization Association promulgated the Technical Regulations of Rectangular Steel Concrete Structures, and dividing it into three types of the joint of rectangular steel concrete structural beams and columns: interior clapboard, outer clapboard and clapboard penetration (2004), e.g. see Fig. 1.1.

Mastui researched the joint of the clapboard throughout of the CFST column and steel beam flange, respectively in 1985 and 1987. They carried static load tests, and knew that this type of joint has a good performance (Matsui, 1985; Kanatani et al, 1987). Ricles performed ten tests of the three types joints of CFST column and H-shaped steel beam, including the interior diaphragms joints, T-steel to strengthen the flange joints, and T-section steel bolts joints, and analyzing the performance of energy dissipation (Ricles et al, 2004). The results showed that interior diaphragms can improve the force performance of the joint. Kubota researched the failure mode of the joint of the clapboard throughout of the CFST column and steel beam (Shin et al, 2004; Kubota et al, 2007). Chen did the research in both theoretical and experimental ways on the CFST column and H-shaped steel beam (Chen et al, 2002; Miao, 2005). Although a lot of researches for the composite structure of the CFST column and steel beam have already done at home and abroad, less paper reported the research on the partitions throughout joint of the CFST column and steel beam in the actual project. It is necessary to take deeper research on the joint of the CFST column and steel beam under cycle loading.

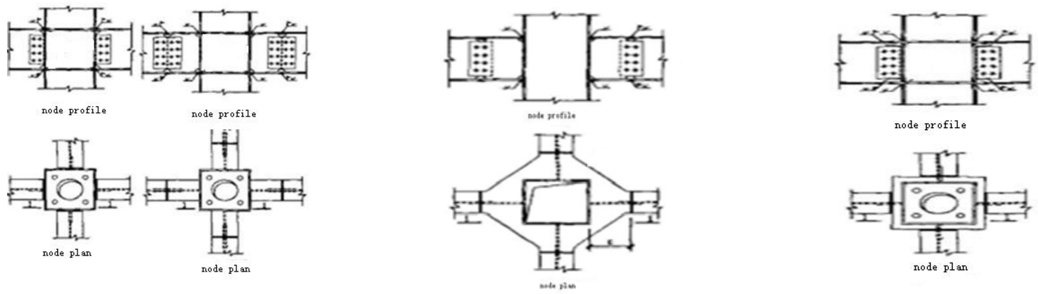

(a) Interior clapboard (b) Outer clapboard (c) Clapboard penetration

Figure 1.1. Joint forms

2. NUMERICAL MODELLING

2.1. Validation of Simulation

Fanning and Tucker performed a numerical simulation for steel flush endplate joints based on Eurocode3 and experimental results. This experiment and numerical simulation was used as an example to compare the results between the experiment and the numerical simulation in the paper to confirm the reliability of the simulation, e.g. see Fig. 2.1.

From the results compared in the above example, we can know that those results are similar to the ones of the experiment. The failure mode and mechanical performance during loading process by using the ANSYS method match well with the results in Fanning's paper. Therefore, the finite element simulation which ANSYS software was used in the paper is reliable and feasible for the numerical simulation of the joints of the CFST column and the steel beam.

2.2. Basic Assumptions

To make the nonlinear finite element analysis, some basic assumptions should be adopted in the paper:

(1) The slips between the square steel tube and core concrete was not considered, and the bonding processing in the FE model was used.

(2) Concrete, steel plate and bolts are homogeneous, their defects are not considered.

(3) When establishing the bolt contacts, the contact between the bolt shank and bolt hole is ignored.

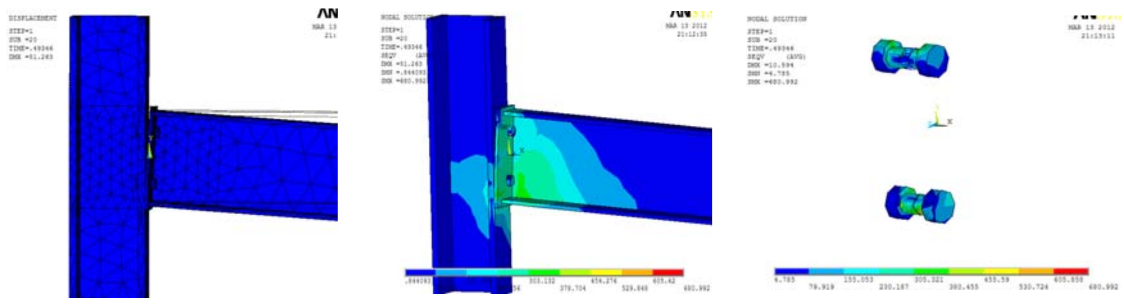

(a) Deformation graph (b) Stress cloud chart (c) Bolt stress cloud chart

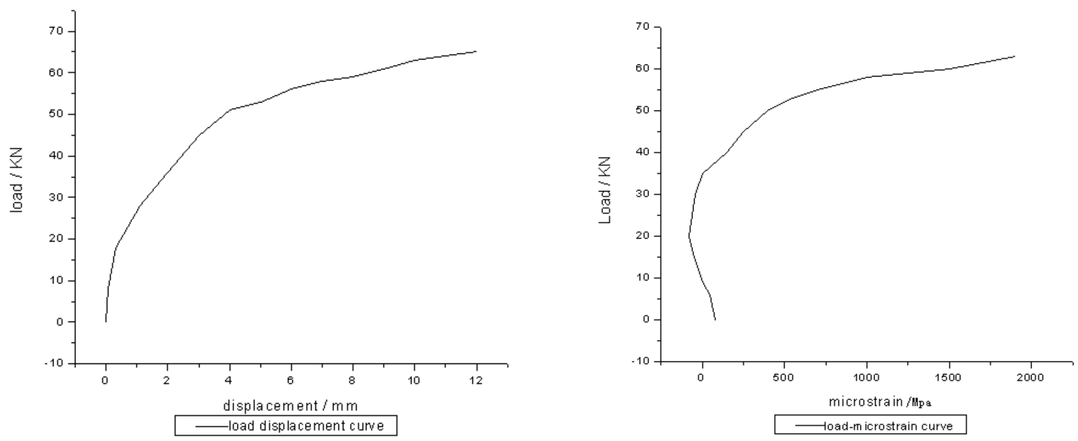

(d) Load-displacement curve (e) Load-microstrain curve

Figure 2.1. Simulation results

2.3. Material Selection

In this paper, based on the actual project, the same dimensions and material properties of the components for the numerical finite element analysis were used, shown in Table 1 and Table 2, respectively. The square steel tube columns and clapboard steel were made of Q345B, and beams and the steel of splice plate were made of Q235B, M22 of 10.9 friction type high strength bolts were used. The concrete grade in the steel pipe was C30. The connections were a hybrid of bolt and weld, e.g. see Fig. 2.2.

The constraint constitutive model of concrete was adopted and the stress-strain relationship of constraint and unconstraint concrete were shown in Figure 2.3(a). Because of outsourcing steel pipe restraints, when the pressure in the concrete close to the uniaxial compressive strength of concrete, the stress – strain of concrete will be greatly improved.

Table 2.1. Component Dimensions

Number	Column size (b×h×H×t) /mm	Clapboard thickness /mm	Clapboard stretch length /mm	Clapboard space /mm	Beam size (l_b×h_w×t_b×t_w) /mm	Beam length /mm
JDA-1	300×300×3000×6	16	25	408	120×400×8×6	900
JDA-2	300×300×3000×6	10	25	402	120×400×8×6	900
JDA-3	300×300×3000×6	16	60	408	120×400×8×6	900
JDA-4	300×300×3000×6	10	60	402	120×400×8×6	900
JDA-5	300×300×3000×6	16	100	408	120×400×8×6	900
JDA-6	300×300×3000×6	10	100	402	120×400×8×6	900

Table 2.2 The parameters of materials

Material type	Yield strength fy /(N/mm^2)	Limit strength fu /(N/mm^2)	Young's modulus Es /(N/mm^2)	Material type	Compressive strength fc /(N/mm^2)	Young's modulus Es /(N/mm^2)
Beam	238	338	2.05×105	concrete	20.1	2.95×104
Column	348	451	2.05×105			
Bolt	917	1040	2.05×105			

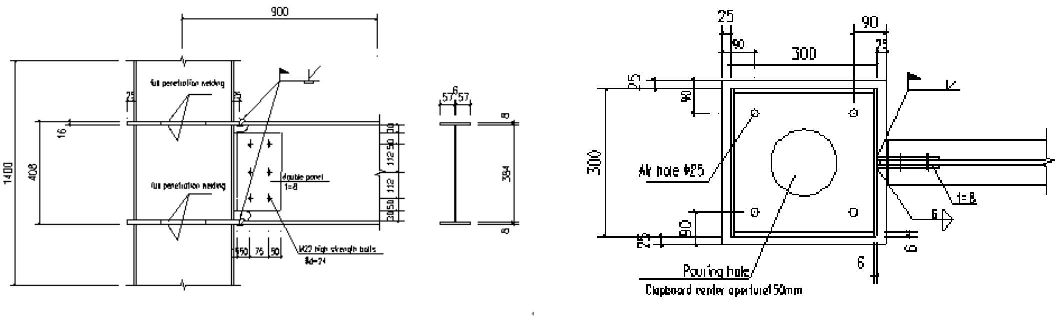

(a) profile (b) plane

Figure 2.2 Component section

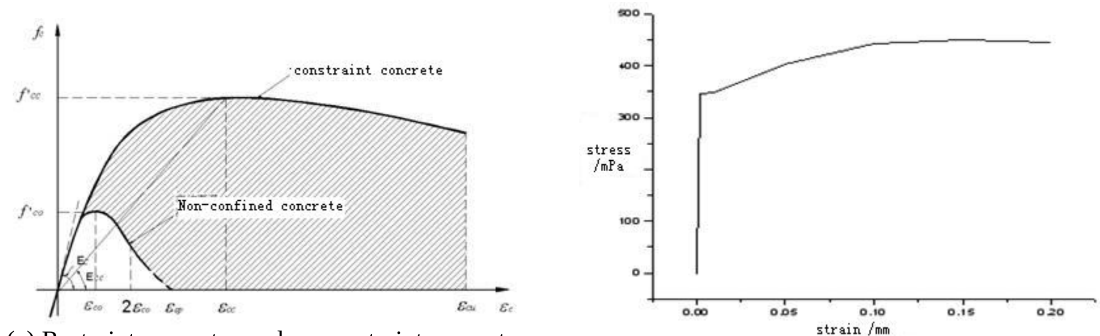

(a) Restraint concretes and non-restraint concrete stress-strain model

(b) Steel stress-strain model

Figure 2.3. Stress-strain relationship

In this paper, the multi-linear constitutive model of steel was used, and the stress-strain relationship of steel was shown in Figure 2.3(b). The constitutive model for the restraint concrete in the square and rectangular steel tube from was described by Han (Han, 2004).

$$y = 2x - x^2 \qquad (x \le 1)$$

(2.1)

$$y = \frac{x}{\beta(x-1)^{\eta} + x} \qquad (x > 1)$$

(2.2)

$$x = \varepsilon / \varepsilon_0$$
$$y = \sigma / \sigma_0$$
$$\sigma_0 = \left[1 + \left(-0.0135\xi^2 + 0.1\xi\right) \cdot \left(24 / f_c\right)\right] \cdot f_c^{'}$$
$$\varepsilon_0 = \varepsilon_{cc} + \left[1330 + 760 \cdot \left(f_c^{'} / 24 - 1\right)\right] \cdot \xi^{0.2} \left(\mu\varepsilon\right)$$
$$\varepsilon_{\mu} = 1300 + 12.5 \cdot f_c^{'} \left(\mu\varepsilon\right)$$
$$\eta = 1.6 + 1.5 / x$$
$$\beta = \begin{cases} \left(f_c^{'}\right)^{0.1} / 1.35\sqrt{1+\xi} & \left(\xi \le 0.3\right) \\ \left(f_c^{'}\right)^{0.1} / 1.35\sqrt{1+\xi \cdot \left(\xi - 2\right)^2} & \left(\xi > 0.3\right) \end{cases}$$

2.4. Finite Element Modelling

The finite element software ANSYS was used in this paper for the simulation analysis on the earthquake resistance performance of the combination joints of the CFST column and H-shaped steel beam. The ANSYS has provided the strong analysis modules, includeing before processing module, solution module and post-processing module.

(1) In the model, all steel products use the Von Mises yield criterion and the multilinear kinematic hardening criterion, and simultaneously consider the Bauschinger effect. For the steel tube column and steel beam which is away from the joint range uses 8-node hexahedron solid element (solid 45), and this element have plasticity, creep, swelling, stress stiffening, large deflection, and large strain capabilities. In the joint range, all the elements use 20 nodes tetrahedron entity (solid 95), and this element has two displacement patterns to make it possible better the simulation anomalous grid and support plasticity, the super-elasticity, the slow change, the stress steel, the big distortion and big strain capacity.

(2) The core concrete uses the 8-node hexahedron solid element (solid 65) recommended by ANSYS, which has crack and crush performance, simulation of concrete cracking, crushing, plastic deformation and creep, and also can simulate the reinforcement tension, compression, plastic deformation and creep, and other properties, respectively. For the concrete uses the elastoplastic constitutive model and W-W five parameter failure criterions. Meanwhile as the simulation analysis focuses on the node territory and the end part of the beam, but the core concretes are at the ideal three bearing condition in the node territory, therefore we neglected the contact slipping between the steel tube and the concrete during the simulation.

(3) In the model, we need to set the contact form and pre-tightening force. The surface to surface contact is used in the paper to deal with the contact between the splice plate and the beam web

plate, the bolt head and the bolt mother and the splice plate. The 6 node triangle target element (TARGE170) and 6 node triangle contact element (CONTA174) are used to carry on the simulation. For the pre-tightening force uses the pre-tightening element (PRETS179) which has provided to carry on the simulation in ANSYS.

(4) For the grid division, we use map and free grid division, which carries on the free detail division in the node range and use the map grid division in the away from node range, e.g. see Fig. 2.4.

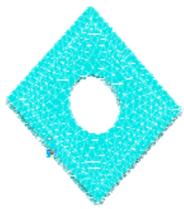

(a) Clapboard grid

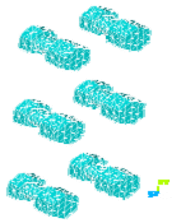

(b) Bolt grid

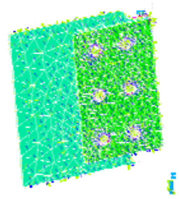

(c) Contact element grid

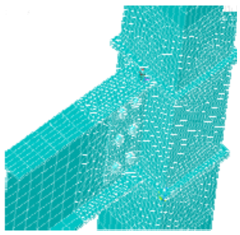

(d) Model grid

(d) Node domain concrete grid

Figure 2.4. Finite element model

2.5. Loading and Solving

(1) In this paper, we use the inflection point of the actual node to simulate. We exert the displacement constraints of X and Y direction on the top of the column, and X, Y, Z three directions displacement constraints on the bottom of the column. As the same time, we exert the Y direction displacement constraint on the loading end of the beam in order to prevent the local instability out of plane in the loading process. The pre-tightening force is applied to the bolt according to the actual construction order at the first, and then the vertical downward centralized load of the Z direction is applied on the coupling node which we had carried on the coupling to the top section of the column. At last, the vertical downward centralized load and the low cyclic loading on the loading end of the beam is applied.

(2) The nonlinear solution using the Newton - Raphson equilibrium iteration method is used in this paper and the pre-placed condition conjugate gradient solution (PCG) is selected. As the same time, the automatic time step and adaptive decline control in order to strengthen the convergence are opened.

3. NONLINEAR FINITE ELEMENT ANALYSIS

3.1. Unidirectional Load Nonlinear Finite Element Analysis

We can know from unidirectional finite element simulation that the destruction of the composite joint mainly occurs on beam's flange, resulting in the destruction by the lower flange compression buckling, e.g. see Fig. 3.1. and Fig. 3.2.

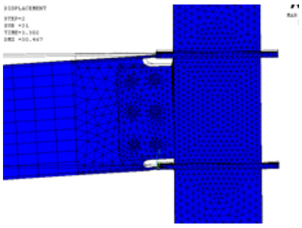

(a) Joint deformation graph

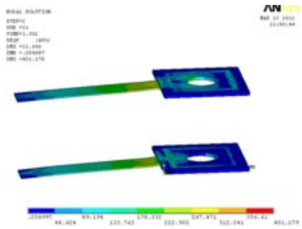

(b) Beam Mises-stress cloud chart

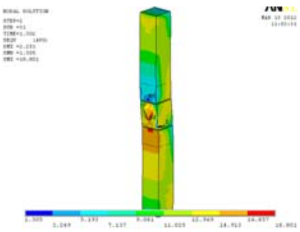

(c) Core-concrete Mises-stress cloud chart

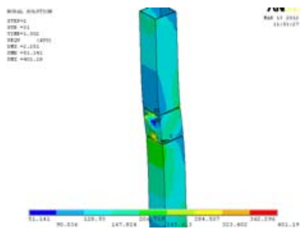

(d) steel tube Mises-stress cloud chart

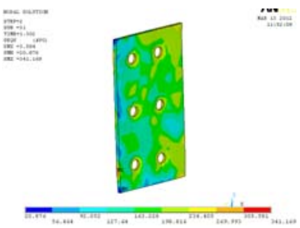

(e) Splice plate Mises-stress cloud chart

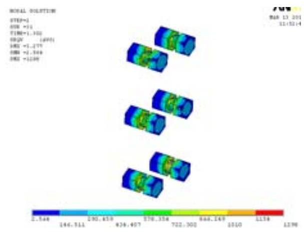

(f) Bolts Mises-stress cloud chart

Figure 3.1. Mises stress cloud chart

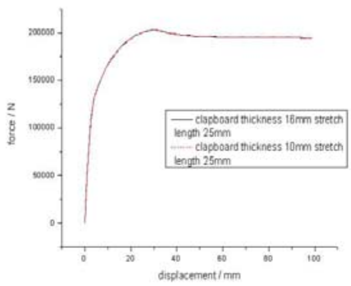

(a) Clapboard stretch length 25mm thickness 16mm and 10mm

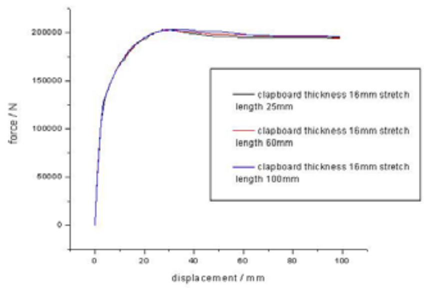

(b) Clapboard thickness 16mm stretch length 25mm, 60mm and 100mm

Figure 3.2. Unidirectional force-displacement curve

Through the finite element analysis, we know that this kind of clapboard penetration type joint has the high bearing capacity, belongs to the rigid joint. We can also know that when the clapboard stretch length is certainly given and the clapboard thickness is changed, it is not too obvious for the node bearing capacity's influence from the contrast above three groups of data. But the thick clapboard's supporting capacity can be slightly higher than the thin one.

Table 3.1. Limit Supporting Capacities

Size	Limit supporting capacities	Size	Limit supporting capacities
Clapboard thickness 10mm and stretch length 25mm	201693 N	Clapboard thickness 16mm and stretch length 25mm	201852 N
Clapboard thickness 10mm and stretch length 60mm	202720 N	Clapboard thickness 16mm and stretch length 60mm	202786 N
Clapboard thickness 10mm and stretch length 100mm	203048 N	Clapboard thickness 16mm and stretch length 100mm	203248 N

Through the contrast of the above two groups of data, we may know that when the clapboard thickness is certainly given, changing the clapboard stretch length will have a certain of influence on the bearing capacity of this kind combination node, but it is not very obvious. Increasing with the clapboard stretch length, the flange’s flexural spot and the plastic region have the offset, causing the beam's destruction region to move to the middle, and preventing from the present of the brittle failure in the steel node root.

3.2. Nonlinear FEA for Reciprocating Cycle Loading

The results of the nonlinear finite element analysis for reciprocating cycle loading are shown in Fig. 3.3. and Fig. 3.4., respectively

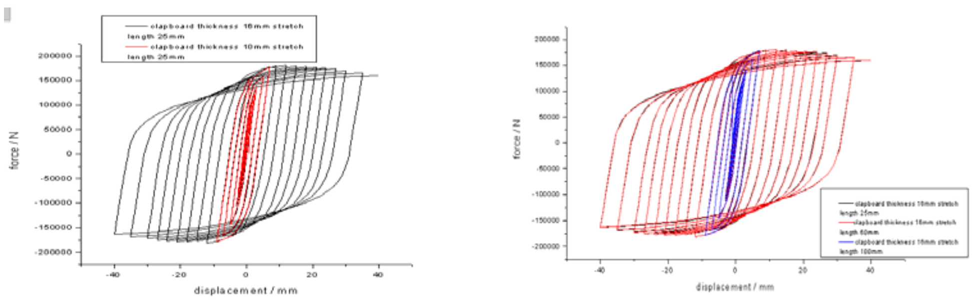

(a) Clapboard stretch length 25mm , thickness 16mm and 10mm

(b) Clapboard thickness 16mm, stretch length 25mm, 60mm and 100mm

Figure 3.3. Hysteretic curves

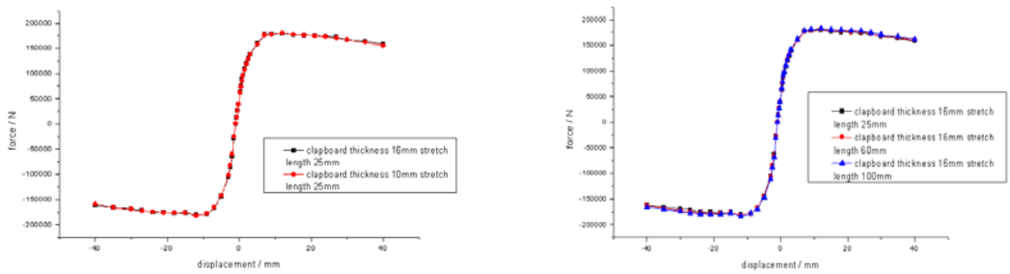

(a) Clapboard stretch length25mm, thickness 16mm and 10mm

(b) Clapboard thickness 16mm, stretch length 25mm, 60mm and 100mm

Figure 3.4. Skeleton curves

Table 3.2. Performance Parameter

Size	Displacement ductility coefficient μ	Equivalent viscous damping coefficient ζ_{eq}	Energy dissipative coefficient E
Clapboard thickness 10mm, stretch length 25mm	4.40	0.27	1.67
Clapboard thickness 10mm, stretch length 60mm	4.54	0.40	2.52
Clapboard thickness 10mm, stretch length 100mm	4.62	0.44	2.77
Clapboard thickness 16mm, stretch length 25mm	4.45	0.28	1.78
Clapboard thickness 10mm, stretch length 60mm	4.57	0.44	2.77
Clapboard thickness 10mm, stretch length 100mm	4.66	0.45	2.81

4. CONCLUSIONS

Through the above analysis, we can conclude that this kind of node has a higher supporting capacity, good ductility and energy dissipation capacity. When changing the clapboard thickness, the clapboard has certain of influence to the node performance. Increasing the clapboard thickness, the ultimate bearing capacity of the node is slightly improved, and the ductility and energy dissipation coefficient are also slightly higher. When increasing the clapboard stretch length, the node limit supporting capacity is rising, and the ductility performance and the energy consumption performance will also be improved. Meanwhile along with increasing of the clapboard stretch length, the flexure destruction position of the beam flange also gradually move away from the node root, and the plastic region will also relocate, and the node performance will be improved.

In this finite element simulation, we did not consider the relative slip between the steel tube and concrete, and this may create slightly different against the actual situation, and it can be improve in the later research.

AKCNOWLEDGEMENT

The reported research was partially supported by Angang Construction Group 2011 Foundation, and the Science and Technology Project of Ministry of Housing and Urban-Rural Development with grant 2011-k2-17.

REFERENCES

Rectangular steel pipe concrete structure technical regulation. (2004). *China Engineering Construction Standardization Association* 27-28.

Matsui. (1985). Strength and behavior of frames with concrete filled square steel tubular columns under earthquake loading. *The International Specialty Conference on Concrete Filled Steel Tubular Structure.* Harbin, China, August.

Kanatani, H., Tabuchi, M., Kamba, T. and Hsiaolien, J. (1987). A study on concrete filled RHS column to H-beam connections fabricated with HT bolts in rigid frames. *Proceedings of the First Composite Construction in Steel and Concrete Conference.* Engineering Foundation: 614-635.

Ricles, J. M., Peng, S. W. and Lu, L. W. (2004). Seismic behavior of composite concrete filled steel tube column-wide flange beam moment connections. *Journal of Structural Engineering*. **130: 2**, 223-232.

Shin, K. J., Kim ,Y. J. (2004). Behavior of welded CFT column to H-beam connections with external stiffeners. *Engineering Structure.* **26: 7**, 1877-1887.

Jun, K., Masaya T., and Kiyoshi, T. (2007). Elasto-plastic behavior of connection between concrete-filled square steel tubular column and steel beam using split external diaphragm. *Annual Report.* Kajima Technical Research Institute, Kajima Corporation. **52: 2**, 65-70.

Chen, Z. H. and Jiang, X. L. (2002). Square steel pipe concretes joint connection bearing strength test research. *Technical Report of Tianjin University.*

Miao, J. K. (2005). Square steel pipe concrete column and H steel girder outside rib link board node research. *Tianjin University master graduation thesis.*

Han, L. H. (2004). Steel pipe concrete structure: theory and practice. Science Press, China.